Combustion, Explosion, and Shock Waves, Vol. 41, No. 4, pp. 435–448, 2005

Numerical Simulation of Formation of Cellular Heterogeneous Detonation of Aluminum Particles in Oxygen

A. V. Fedorov[1] **and T. A. Khmel'**[1]

UDC 532.529+541.126

Translated from *Fizika Goreniya i Vzryva*, Vol. 41, No. 4, pp. 84–98, July–August, 2005.
Original article submitted July 5, 2004.

Formation of cellular detonation in a stoichiometric mixture of aluminum particles in oxygen is studied by means of numerical simulation of shock-wave initiation of detonation in a flat and rather wide channel. By varying the channel width, the characteristic size of the cells of regular uniform structures for particle fractions of 1–10 μm is determined. The calculated cell size is in agreement with the estimates obtained by methods of an acoustic analysis. A relation is established between the cell size and the length of the characteristic zones of the detonation-wave structure (ignition delay, combustion, velocity and thermal relaxation).

Key words: gas suspensions, cellular detonation, numerical simulation.

INTRODUCTION

It is commonly known that the widely used Zel'dovich–Neumann–Döring model of detonation is an excellent ideal approximation but does not describe all specific features of propagation of real detonation waves. Because of instability of the plane front to spatial fluctuations, the propagation regime acquires the form of multifront or cellular detonation. In this case, the detonation front consists of segments of overdriven and decaying detonation waves converging in triple points where transverse waves are also generated. The system of transverse waves moving in the opposite directions is regular, and the trajectories of triple points during front propagation form a pattern consisting of diamond-shaped cells. The mechanisms that ensure the cellular character of detonation play an important role in the deflagration-to-detonation transition in bounded volumes and in passage of detonation into an open space. Problems of cellular detonation in gas mixtures have been discussed in many papers (see the reviews [1–4]).

One important aspect of cellular detonation is establishing relations between the cell size and detonation parameters. The basic geometric scales characterizing the chemical processes in the detonation wave are the lengths of the induction zone (ignition delay) and combustion zone. An analysis of the first results, which made it possible to get a general idea about the relation of the transverse or longitudinal cell size (a or b, respectively) with physical and chemical properties of a gas mixture, can be found in the review [2]. The linear dependence of the cell size on the induction-zone length [$a = k\lambda$, where $\lambda = (D_0 - u)\tau$] was first established in [5] in the approximation of the reaction zone consisting of the induction zone and the front of instantaneous heat release, which agrees with the specific features of detonation combustion of gas mixtures. (Here, D_0 is the detonation-front velocity, u is the gas velocity behind the front, τ is the induction time, and k is the proportionality coefficient.) Subsequent investigations confirmed the conclusion that the mechanisms responsible for instability operate in the heat-release zone [1]. The estimate of the cell size on the basis of the conditions of flameout behind a diverging cylindrical front yields the relation between the transverse cell size and the induction-zone length in the form $b \approx (E_a/(RT))D_0\xi\tau_0$, where E_a is the activation energy, R is the universal gas constant, T is the temperature, τ_0 is the induction time, and ξ is a constant whose value ($0.5 < \xi < 2$) depends on the choice of the flameout criterion [6]. A similar dependence of the cell size on the induction-zone

[1]Institute of Theoretical and Applied Mechanics, Siberian Division, Russian Academy of Sciences, Novosibirsk 630090; khmel@itam.nsc.ru.

length was obtained in [7] within the framework of a generic model of the detonation cell, where the collision of transverse waves is considered as a microexplosion with an instantaneous reaction zone. The linear law of cell-size variation as a function of the induction-zone length was also derived by processing experimental observations of cellular structures of overdriven detonation [8]:

$$\frac{\lambda}{\lambda_{\mathrm{CJ}}} = \frac{L_{\mathrm{ind}}}{L_{\mathrm{CJ}}} = \frac{D}{D_{\mathrm{CJ}}} \exp\left\{\frac{E_{\mathrm{a}}}{RT_{\mathrm{ZND}}}\left[\left(\frac{D_{\mathrm{CJ}}}{D}\right)^2 - 1\right]\right\}.$$

Here, λ is the characteristic transverse cell size, L_{ind} is the induction-zone length, D is the front velocity, the subscript "CJ" indicates the Chapman–Jouguet wave, and T_{ZND} is the temperature at the front in the Zel'dovich–Neumann-Döring model. Obviously, the first part of the relation is not universal, because both the detonation velocity and the parameters in the chemical spike region and in the equilibrium state change as the detonation becomes more overdriven.

Thus, in the approaches described above, the cell size is related to the induction-zone width, which is the governing parameter in the gas-detonation wave structure. As was indicated in [2], the dependence becomes more complicated if the finite size of the heat-release zone is taken into account.

Barthel [9] involved not only the induction zone but also the combustion zone to estimate the detonation-cell size. The transverse cell size (distance between the neighboring transverse waves following in the same direction) is determined by analyzing the propagation of acoustic fluctuations in the flow field behind the steady detonation front. The cell size calculated for the basic flow field of the Chapman–Jouguet wave are substantially greater than those observed in experiments. Consideration of moderately overdriven waves, however, made it possible to approach the experimental data and to reach qualitative agreement with variation of the initial pressure and composition of gas mixtures.

The studies [10, 11] confirm the influence of the heat-release zone on the detonation-cell size. The results of measurements of the cell sizes in hydrogen–air mixtures with addition of carbon dioxide and the zone sizes calculated by models with allowance for detailed chemical kinetics and characterizing the processes of the chemical reaction (induction and combustion) on the basis of different criteria were analyzed in [10]. It was found from the results with a varied composition of the mixtures that the dependence between the cell size and the induction and combustion zones is more complicated than the linear one. The relation between the lengths of the characteristic reaction zones determined with the use of detailed chemical kinetics in the one-dimensional Zel'dovich–Neumann–Döring model and the cell size observed experimentally and obtained numerically within the framework of the model with reduced single-step chemical kinetics was established in [11]. This relation is characterized by two parameters. One of them determines the measure of sensitivity of the reaction zone to variation of initial conditions (shock-wave amplitude), and the second one is related to the ratio of heat release of the chemical reaction to the initial thermal energy.

The relation between the cell size and the lengths of the induction and combustion zones was experimentally validated in the case of detonation of heterogeneous mixtures with a more complicated structure. Observations of cellular hybrid detonation in a hydrogen–air mixture with addition of aluminum powder [12, 13] showed that the presence of aluminum particles can exert the opposite effects on the characteristics of gas detonation, depending on the particle size. Thus, addition of fine spherical particles and flakes increases the detonation velocity and decreases the characteristic cell size. Addition of coarse particles, vice versa, leads to a decrease in the detonation velocity and to an increase in the cell size, as compared to gas detonation. Apparently, the reason is that the effect of the aluminum ignition and combustion processes on the detonation parameters becomes more and more pronounced as the particle concentration increases. Therefore, the presence of rapidly igniting and rapidly burning (fine or flake-type) or slowly igniting and slowly burning (coarse) particles leads to the opposite effects.

The degree of influence of the scale of the induction and heat-release (combustion) zones on the characteristics of cellular detonation can be determined more accurately for media in which these scales are commensurable in the order of magnitude. In particular, such mixtures include suspensions of reacting particles in air or oxygen, where the combustion duration is normally longer than the ignition delay. Detonation flows in disperse media are also characterized by interphase interaction; hence, they have additional scales determined by the length of the zones of velocity and thermal relaxation of the phases. It is of much interest to which extent these scales can affect the cellular detonation structures being formed.

The process of cellular heterogeneous detonation in suspensions of aluminum particles in gases has not been adequately studied. Several cellular-type structures 5–10 cm in size were registered in the experiments [14] on detonation initiation in a mixture of aluminum particles and oxygen in an unbounded cloud. These structures were observed at the outer boundary of the cloud; hence, it is doubtful that they will exist at the next stage of wave propagation. The deflagration-

to-detonation transition in suspensions of starch, anthraquinone, and aluminum particles in air were considered in [15]. The data on the pressure distribution in the detonation wave in a suspension of aluminum flakes indicate the presence of transverse waves typical of cellular detonation, where the characteristic cell size is ≈0.4 m.

One method successfully used to study detonation processes, including cellular detonation, is numerical simulation, which allows one to identify the detailed flow pattern and determine the qualitative and quantitative dependences of dynamic and geometric characteristics on initial parameters. Results of numerical simulations of cellular structures of hybrid detonation of a hydrogen–oxygen mixture with aluminum particles are described in [16]. An analysis of the cell size calculated for a varied content of particles in the mixture showed that the dependence of the cell size on the detonation velocity in the case of addition of fine particles is in good agreement with the formula derived in [12] for overdriven detonation. For coarse aluminum particles ($d = 13$ μm), this dependence is valid only if the content of particles is low.

Cellular heterogeneous detonation of a lean gas suspension of fine aluminum particles ($d = 1$ and 2.5 μm) was numerically simulated in [17]. Oxygen was considered as a carrier gas. The calculated detonation velocity for the accepted value of the initial concentration of particles, corresponding to the stoichiometric value in air, is in line with the corresponding results of [18]. Computations on adaptive grids with high resolution revealed a detailed pattern of the two-dimensional structure of the cellular detonation flow. The calculated cell size was 6 cm for 2.5-μm particles, and transitional structures with the cell size ranging from 1.1 to 1.4 cm were obtained for particles 1 μm in diameter.

The experience of numerical simulations of two-dimensional flows of gas detonation shows that the cellular structure depends on the size of the computational domain [19] and that there exist transitional structures with a varied character of regularity and cell size [20]. To determine the size of the cellular structure proper, one has to eliminate the influence of the boundary conditions. Calculations in the domain with the transverse size of the order of one cell involve an additional length scale, which relates the cell size to the domain width [19]. The cell size is determined most accurately in domains containing a large number of cells as the ratio of the domain width to the number of cells over the cross section.

In the present paper, we find numerically the characteristic size of the structure of cellular detonation in a suspension of aluminum particles in oxygen for different fractions of particles. With allowance for the results of [19], the computations were performed for channels containing several cells, and the cell size was determined on the basis of data for uniform regular structures. The size of characteristic zones (velocity and thermal relaxation, ignition delay, and combustion) in a heterogeneous mixture depend on the particle size, whereas the front velocity and the amplitude characteristics of detonation can be considered as invariable. The objective of the present work was to find the dependence between the detonation-cell size and the scales characterizing the dynamic and chemical processes in the heterogeneous detonation wave structure. The numerical results are compared with the cell size estimated by an acoustic analysis [9].

The mathematical model of detonation of aluminum particles in oxygen, which was verified against the experimental data of [21], was developed in [22–24] and used in [25–27]. The model is based on representations of a two-velocity two-temperature continuum of mechanics of heterogeneous media. Aluminum combustion is described by a reduced reaction initiated when the particle reaches a certain critical temperature (ignition temperature) with allowance for incomplete combustion of particles, which is caused by the growth of an oxide film preventing combustion. The values of the initial parameters (ignition temperature, activation energy, heat release, and chemical reaction rate) were determined with allowance for their correspondence to available experimental data on the detonation velocity and the size of the ignition-delay and combustion zones. The dependence of the velocity of steady detonation on the particle concentration was accepted in accordance with the data of [21]. The characteristic time of aluminum-particle combustion in oxygen agrees with the data of [28]. The ignition temperature, determining the induction time, was set to be close or equal to the value accepted in [18]. A theoretical analysis of steady detonation structures was performed in [24]; the calculated parameters in the Chapman–Jouguet plane were in agreement with the experimental data of [21] on pressure and concentration of unburnt particles. A numerical study of one-dimensional and two-dimensional problems of shock-wave initiation within the framework of the model described in the present paper was performed in [25–27]; the results of [25, 26] are in good agreement with experimental and numerical data of [18] on the initiation energy. By virtue of the aforesaid, it seems reasonable to use this model to study cellular detonation in a suspension of aluminum particles in oxygen and to obtain qualitative and quantitative characteristics of cellular structures.

PHYSICAL AND MATHEMATICAL FORMULATION OF THE PROBLEM

We consider a cloud of a single-fraction homogeneous suspension of spherical aluminum particles in oxygen with a concentration close to the stoichiometric value (1.34 kg/m^3), which fills the half-space of an infinite flat channel over its entire width. The process of formation of the cellular structure is modeled as a result of development of fluctuations arising in the case of shock-wave initiation of detonation in the gas suspension. The initiator is assumed to be a plane shock wave (SW) propagating along the channel over the pure gas (oxygen) and accompanied by a rarefaction wave. Thus, the physical formulation of the problem is a two-dimensional extension of [26] or a particular case of the model developed in [27], if the reacting mixture fills the entire cross section of the channel. If the amplitude and the energy stored are sufficiently high [26, 27], an overdriven detonation wave is formed in the cloud, which is attenuated by the rarefaction wave and reaches the self-sustained detonation mode. The transversely nonuniform initial fluctuation of the particle density in a short region adjacent to the leading edge of the cloud plays the role of the initiator of small fluctuations.

The equations that describe the flow of a two-phase mixture in the two-velocity two-temperature approximation of mechanics of heterogeneous media express the laws of conservation of mass, momentum, and energy of each phase:

$$\frac{\partial \rho_i}{\partial t} + \frac{\partial \rho_i u_i}{\partial x} + \frac{\partial \rho_i v_i}{\partial y} = (-1)^{i-1} J,$$

$$\frac{\partial \rho_i u_i}{\partial t} + \frac{\partial [\rho_i u_i^2 + (2-i)p]}{\partial x} + \frac{\partial \rho_i u_i v_i}{\partial y} = (-1)^{i-1}(-f_x + J u_2),$$

$$\frac{\partial \rho_i v_i}{\partial t} + \frac{\partial (\rho_i u_i v_i)}{\partial x} + \frac{\partial [\rho_i v_i^2 + (2-i)p]}{\partial y} = (-1)^{i-1}(-f_y + J v_2), \tag{1}$$

$$\frac{\partial \rho_i E_i}{\partial t} + \frac{\partial [\rho_i u_i (E_i + (2-i)p/\rho_1)]}{\partial x} + \frac{\partial [\rho_i v_i (E_i + (2-i)p/\rho_1)]}{\partial y} = (-1)^{i-1}(-q - f_x u_2 - f_y v_2 + J E_2).$$

Here p is the pressure, $\rho_i = m_i \rho_{ii}$, u_i, v_i, E_i, and $c_{v,i}$ are the mean density, streamwise and transverse velocity components, total energy per unit mass, and heat capacity of the ith phase ($i = 1, 2$), m_i is the volume concentration, and ρ_{ii} are the true densities of the phases; the subscripts 1 and 2 refer to the gas and particles, respectively. The system is closed by the equations of state (in the approximation of a low volume concentration of particles)

$$p = \rho_1 R T_1, \;\; E_i = \frac{u_i^2 + v_i^2}{2} + c_{v,i} T_1 + (i-1)Q \tag{2}$$

and by the reduced equation of the chemical reaction

$$J = \frac{\rho}{\tau_\xi} \max(0, (\xi - \xi_k)) \exp\Big(-\frac{E_\mathrm{a}}{R T_2}\Big), \;\; T_2 \geqslant T_\mathrm{ign}; \qquad J = 0, \quad T_2 < T_\mathrm{ign}. \tag{3}$$

Here T_1 and T_2 are the gas and particle temperatures, respectively, Q is the heat release due to the chemical reaction, $c_{v,1}$ and $c_{v,2}$ are the heat capacities of the gas and particles, respectively, $\xi = \rho_2/\rho$ is the relative mass concentration of particles, $\rho = \rho_1 + \rho_2$, E_a is the activation energy, ξ_k is the concentration of the solid phase at the Chapman–Jouguet point (unburnt particles with condensed aluminum oxide), T_ign is the ignition temperature, and τ_ξ is the characteristic burning time. The mathematical model (1)–(3) is semi-empirical and contains constants determined from the condition of their agreement with experimental data. The quantity Q characterizing the integral heat release of the chemical reaction is set in a manner that ensures the agreement with the data of [21] on the detonation velocity as a function of the particle concentration. The interphase interaction is determined by the formulas

$$\boldsymbol{f} = \frac{3 m_2 \rho_{11}}{4d} c_D |\boldsymbol{u}_1 - \boldsymbol{u}_2| (\boldsymbol{u}_1 - \boldsymbol{u}_2), \qquad q = \frac{6 m_2 \lambda_1}{d^2} \mathrm{Nu}(T_1 - T_2); \tag{4}$$

$$c_D(\mathrm{Re}, \mathrm{M}_{12}) = \Big(1 + \exp\Big(-\frac{0.43}{M_{12}^{4.67}}\Big)\Big) \times \Big(0.38 + \frac{24}{\mathrm{Re}} + \frac{4}{\sqrt{\mathrm{Re}}}\Big); \tag{5}$$

$$\mathrm{Nu} = 2 + 0.6 \mathrm{Re}^{1/2} \mathrm{Pr}^{1/3}, \qquad \mathrm{Re} = \frac{\rho_{11} d |\boldsymbol{u}_1 - \boldsymbol{u}_2|}{\mu}, \qquad \mathrm{M}_{12} = \frac{|\boldsymbol{u}_1 - \boldsymbol{u}_2| \sqrt{\rho_{11}}}{\sqrt{\gamma_1 p}}. \tag{6}$$

Here d is the particle diameter, c_D is the drag coefficient of particles, λ_1 is the thermal conductivity of the gas, Re, Nu, Pr, and M are the Reynolds, Nusselt, Prandtl, and Mach numbers, respectively, and μ is the gas viscosity. Formula (5) for the drag coefficient is taken in the form used in [29] because it ensures agreement with

experimental data on the trajectories of particle motion behind transient shock waves.

The initial-boundary problem for system (1)–(6) is formulated as follows:

$$t=0:\quad \varphi=\begin{cases}\varphi_{\text{left}},\ 0\leqslant x<X_{\text{left}},\\ \varphi_{\text{RW}}(x),\ X_{\text{left}}\leqslant x<X_{\text{right}},\\ \varphi_{\text{SW}},\ X_{\text{right}}\leqslant x<X_{\text{SW}},\\ \varphi_{\text{g0}},\ X_{\text{SW}}\leqslant x<X_{\text{cloud}},\\ \varphi_{\text{fluc}}(y),\ X_{\text{cloud}}\leqslant x<X_{\text{fluc}},\\ \varphi_0,\ X_{\text{fluc}}\leqslant x<+\infty,\end{cases} \tag{7}$$

Here $\varphi=\{\rho_1,\rho_1u_1,\rho_1v_1,\rho_1E_1,\rho_2,\rho_2u_2,\rho_2v_2,\ \rho_2E_2\}$ is the vector of the solution, φ_{SW} is the state at the SW front in the gas, $\varphi_{\text{RW}}(x)$ is the profile of the centered rarefaction wave connecting the states φ_{left} ($p=p_0$) and φ_{SW}, X_{left} and X_{right} are the left and right boundaries of the rarefaction wave, X_{SW} is the initial position of the front of the incident SW, φ_{g0} is the state upstream of the SW front in the gas, φ_0 is the initial state of the mixture in the cloud, X_{cloud} determines the frontal boundary of the cloud, X_{fluc} is the coordinate of the boundary of the fluctuating layer, $X_{\text{fluc}}-X_{\text{cloud}}$ is the width of the fluctuating layer, $\varphi_{\text{fluc}}(y)$, $0\leqslant y\leqslant Y$, determines the fluctuating state of the mixture in this layer, and Y is the width of the channel (computational domain).

The boundary conditions on the channel walls were set in accordance with the no-slip and thermal insulation conditions: $\partial\varphi/\partial y=0$. The left boundary of the domain ($x=0$) was subject to "soft" boundary conditions: $\partial\varphi/\partial x=0$. At the right boundary, which was always at a certain distance ahead of the shock (detonation) front, we assumed that $\varphi=\varphi_0$.

The initial values of the parameters of the mixture were taken the same as in [26, 27]: $p_0=1$ atm and $T_0=300$ K. The initial mass concentration of particles was $\xi_0=0.55$, which corresponds to $\rho_{20}=1.34$ kg/m^3. The particle size was varied from 1 to 12 μm. The characteristic burning time τ_ξ was set in the form [28] $\tau_\xi=\tau_0(d/d_0)^2$, where $\tau_0=0.0024$ msec and $d_0=10$ μm. The calculated duration of combustion of a particle 10 μm in diameter was $\approx$0.07 msec for $E_{\text{a}}=10^6$ J/(kg$\cdot$K). This agrees (with allowance for the quadratic dependence on the diameter) with the data on combustion of aluminum particles in pure oxygen [28].

The parameters of the initial profile of the initiating SW were chosen in a manner that ensured detonation-initiation conditions in the cloud of the mixture [26, 27]. The fluctuation initiating the development of transverse waves was set in the form

$$\rho_{2,\text{fluc}}(x,y)=\rho_{20}(1+\beta\cos(n\pi y/Y)). \tag{8}$$

(It was assumed in computations that $\beta=0.1$, $X_{\text{fluc}}-X_{\text{cloud}}=0.01$ m, and $n=1$.)

The computations were performed on a uniform finite-difference grid. The computational domain expanded in the x direction as the leading front propagated over the mixture and included a small portion of the undisturbed flow. A TVD scheme was used to calculate the gas phase [30]. For the discrete phase, some computations were performed by the MacCormack scheme (scheme 1) and some computations were performed by the Gentry–Martin–Daly scheme (scheme 2) (one-dimensional implementations of these schemes can be found in [31]). The results of testing the method in problems of one-dimensional and two-dimensional detonation are described in [32]. Scheme 2 demonstrated a higher efficiency, especially in computing two-dimensional detonation flows, in terms of both the accuracy on the same finite-difference grid and the computation time. The parameters of the finite-difference grid were chosen in accordance with the particle size responsible for the lengths of combustion and relaxation zones. The number of grid nodes over the width of the detonation-wave structure was 50 to 200. In some computation variants, results obtained on nested grids and with varied parameters β and n in Eq. (8) were compared.

FORMATION OF THE CELLULAR STRUCTURE IN DETONATION INITIATION

In numerical simulations of cellular detonation, the initial conditions are normally assumed to be the flow behind a plane steady detonation wave with imposed fluctuations that initiate transverse waves. Travelling of these waves, their reflection from the domain boundaries, and their interaction lead to formation of a cellular structure during further propagation of the front. In the present work, cellular detonation is developed in the course of formation and propagation of a detonation wave in a cloud of suspended particles as a result of shock-wave initiation. The imposed nonuniformity favors origination of weak fluctuations in the flow, which first have an acoustic character and then, with stabilization and propagation of the detonation wave, are transformed to transverse waves of finite amplitude. Formation of the cellular structure occurs on the background of detonation-flow development, which determines the natural character of the cell obtained in computations. Numerical experiments performed with difference values of the amplitude and wavelength of fluctuations show that the geometric size of the regular structure formed is independent of initial parameters of initiation (amplitude and profile of the initiating attenuated SW,

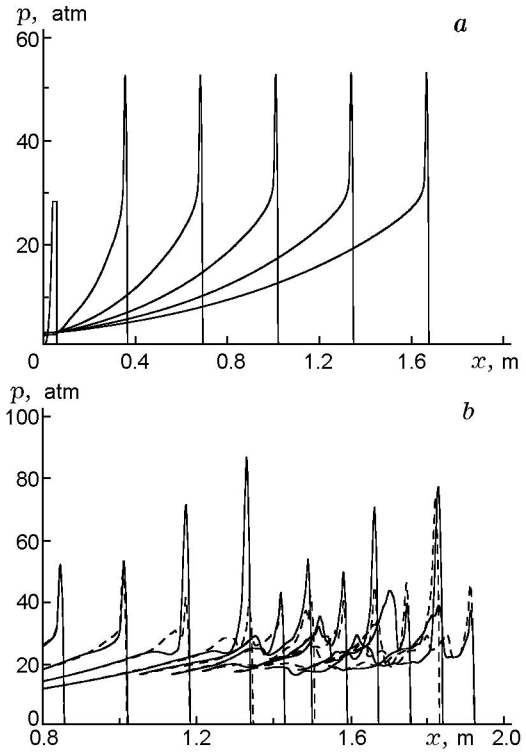

Fig. 1. Detonation formation in one-dimensional problem (a) and two-dimensional problem (b): the solid and dashed curves refer to $y = 0$ and $y = 0.003$ m, respectively.

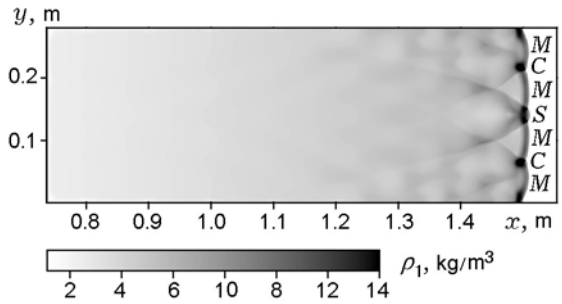

Fig. 2. Instantaneous flow pattern in the two-dimensional problem (gas density).

amplitude and mode of fluctuations, and position of the cloud boundary).

The scenarios of formation of plane detonation waves in the case of SW interaction with a cloud of aluminum particles suspended in oxygen were numerically studied within the framework of the present model in [26]. A typical picture of detonation stabilization in the one-dimensional problem for a mixture with 5 μm particles is shown in Fig. 1a in the form of pressure profiles with a step of 0.2 msec. The chosen values of

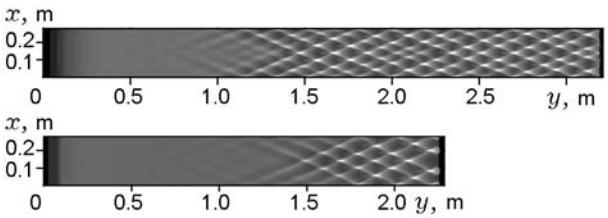

Fig. 3. Formation of nonuniform structures in different types of the difference scheme: results obtained by scheme 1 and scheme 2 are shown at the top and bottom of the figure, respectively.

the amplitude and stored energy of the initiating SW with a trapezium-shaped initial profile provides moderate overcompression of the detonation wave formed and ensures rapid transition to the steady-state mode. The velocity of steady detonation is $D = 1.56$ km/sec. Figure 1b shows similar pressure profiles on the lower wall of the channel ($y = 0$; solid curves) and in the cross section $y = 0.003$ m (dashed curves) in the two-dimensional computation by scheme 1 with $Y = 0.28$ m and $\Delta t = 0.1$ msec up to the time of 0.8 msec and then with $\Delta t = 0.05$ msec. Until the time of 0.6 msec, the fluctuations are small, and the pattern is almost the same as the stabilization of the plane detonation wave in the one-dimensional formulation. Subsequent propagation of the wave acquires an unsteady character. The two-dimensional flow pattern plotted in Fig. 2 in the form of the gas-density distribution at the time $t = 0.9$ msec shows that this phenomenon is caused by the development of cellular detonation, though the structure is not ideally uniform. The points C correspond to collisions of transverse waves, and the segment S in the center of the figure is an overdriven detonation wave: here, the collision of the triple points has already occurred and the transverse waves diverge. The segments M correspond to Mach stems, where the transition from overdriven to decaying detonation occurs at the time discussed. Thus, a structure with 4 cells with a mean transverse size equal to 7 cm is formed in this variant.

DEPENDENCE OF RESULTS OF CELLULAR STRUCTURE FORMATION ON THE WIDTH OF THE COMPUTATIONAL DOMAIN AND GRID PARAMETERS

The influence of the width of the computational domain, finite-difference scheme, and grid parameters on the results of formation of cellular heterogeneous detonation is in line with the known features of cellular

gas detonation [19]. In channels whose width is smaller than a certain critical value, the detonation-wave front remains plane, as in the one-dimensional problem. As the channel width increases (with a fixed particle size), there appears a regular structure whose size is half a cell. Further variation of the channel width generates bifurcation of the structure; as a result, one cell over the channel width is formed. Structures containing half a cell or one cell over the channel width are always regular, i.e., the number of cells over the channel width remains unchanged in the course of propagation of the cellular detonation front. A further increase in the channel width involves further bifurcations, in which the structures become more complicated and their character is changed. In wider channels, the structure near the bifurcation points (where a small increase in the channel width leads to a jumplike change in the number of cells) are irregular and are characterized by fragmentation and coalescence of cells. In regions between the bifurcation points, the structure are regular but can contain cells of different sizes; we will call them nonuniform structures. The degree of nonuniformity can be determined as the ratio of the minimum and maximum cell sizes: $\psi = \lambda_{\min}/\lambda_{\max}$ (λ is the transverse size of the cell). An example of a nonuniform cellular structure is shown in Fig. 2 and in the upper part of Fig. 3 for particles with $d = 5$ μm and channel width $Y = 0.28$ m, where $\psi \approx 2$. The computations show that the structure between the bifurcation points is equidimensional ($\psi = 1$) for a certain value of the channel width.

A comparison of results computed on different grids (including nested grids) with the use of scheme 1 (TVD/MacCormack) and scheme 2 (TVD/Gentry–Martin–Daly) revealed the following. For the channel width close to the bifurcation value (the structure is irregular or nonuniform), the computation results depend significantly on the type of the chosen scheme and grid resolution. Figure 3 shows the results computed for particles with $d = 5$ μm for $Y = 0.28$ m by schemes 1 and 2 on a grid with a step $\Delta x = 0.001$. Different numbers of cell over the channel width were obtained, and their nonuniformity testifies that the channel width is not multiple to the true cell size. A change in the grid step has a similar effect. For instance, the computations by scheme 2 with $\Delta x = 0.005$ m and $\Delta x = 0.004$ m for particles with $d = 8$ μm and $Y = 0.25$ m predict the formation of the structure with one cell over the channel width and one cell and a half over the channel width, respectively. Reproducible results are obtained by computations on substantially finer grids, but the cell size cannot be reliably determined because the structure is irregular or nonuniform.

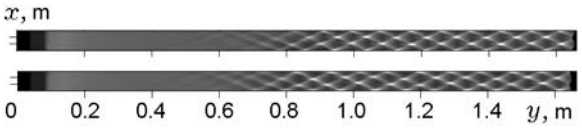

Fig. 4. Results of computations on nested grids with a multiplicity of 2: $d = 3$ μm, $Y = 0.06$ m, $\Delta x = 0.0005$ (at the top) and 0.001 m (at the bottom).

If the structure formed is regular and uniform (or close to uniform, $\psi \approx 1$–1.5), the computations on different grids considered (including nested grids) with the use of two finite-difference methods mentioned above reproduce the same number of cells over the channel width. A decrease in the step of the computational grid provides an increase in accuracy of representation of the detailed flow structure and retains the character of the structure. An example of computations performed by scheme 2 on nested grids with a multiplicity of 2 ($\Delta x = 0.0005$ and $\Delta x = 0.001$ m, $d = 3$ μm, and $Y = 0.06$ m) is shown in Fig. 4.

Thus, the size of the detonation cell can be determined in numerical simulations of regular uniform structures on a comparatively coarse grid containing 50–100 nodes per cell width.

DETERMINATION OF THE DETONATION-CELL SIZE

The characteristic size of the detonation cell is determined by comparing the calculated results on formation of regular structures in channels containing more than two cells. Bifurcation points of the structure allow one to determine the upper and lower limits of the characteristic size of the detonation cell. As the channel width increases, the difference between the limits decreases, and the cell size approaches the mean value. As was noted above, the degree of nonuniformity of regular structures changes if the channel width is varied in the vicinity of this value. The reliable value of the cell size is assumed to correspond to equidimensional structures ($\psi \approx 1$). For nonuniform regular structures, the mean value of the transverse cell size can be defined as the ratio of the channel width to the number of cells formed.

Figure 5 shows the results calculated by scheme 2 with a varied channel width for particle fractions of 10 μm (Fig. 5a; $\Delta x = 0.004$ m) and 7 μm (Fig. 5b; $\Delta x = 0.002$ m). A structure with 3.5 cells and the degree of nonuniformity $\psi \approx 2$ is formed for $Y = 1$ m (at the top of Fig. 5a), a structure with 4.5 cells close to uniform ($\psi \approx 1.25$) is observed for $Y = 1.2$ m (at

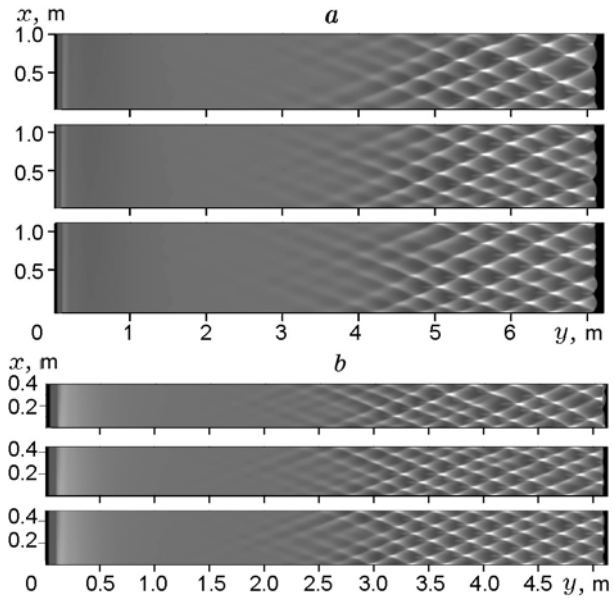

Fig. 5. Formation of nonuniform irregular structures: (a) $d = 10$ μm, $\Delta x = 0.004$ m, and $Y = 1$, 1.1, and 1.2 m; (b) $d = 7$ μm, $\Delta x = 0.002$ m, and $Y = 0.4$, 0.45, and 0.5 m.

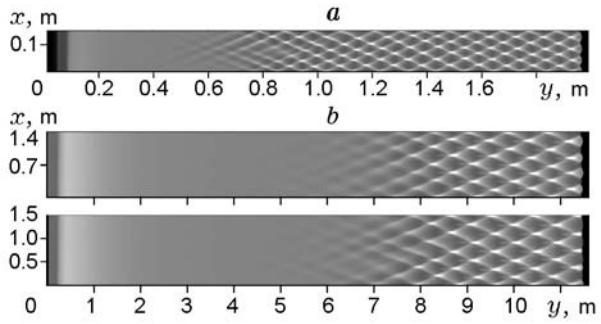

Fig. 6. Formation of uniform regular structures: (a) $d = 3$ μm, $\Delta x = 0.001$ m, and $Y = 0.15$ m; (b) $d = 12$ μm, $\Delta x = 0.005$ m, and $Y = 1.4$ and 1.5 m.

the bottom of Fig. 5a), and a structure with 4.5 cells and the degree of nonuniformity $\psi \approx 1.7$ is formed for $Y = 1.1$ m (in the middle). The bifurcation point is located between 1 and 1.1 m; correspondingly, the cell size for particles with $d = 10$ μm lies in the interval of 24.4–28.5 cm. Similar data for particles with $d = 7$ μm are plotted in Fig. 5b. Here, a nonuniform ($\psi \approx 2$) structure with 2.5 cells is formed for $Y = 0.4$ m, an irregular structure is observed for $Y = 0.45$ m, and an almost uniform ($\psi \approx 1.3$) structure with 3.5 cells is formed for $Y = 0.5$ m. The bifurcation point is close to $Y = 0.45$ m, and the cell size lies in the interval of 12.8–16 cm.

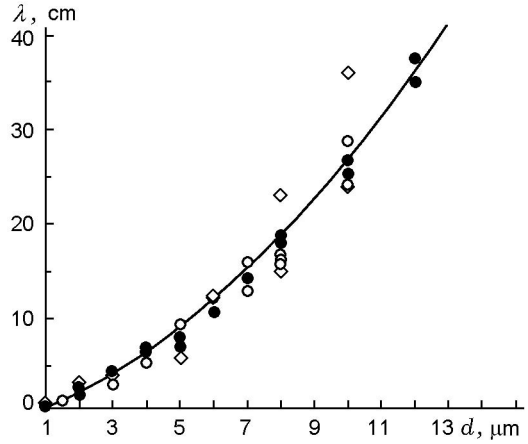

Fig. 7. Calculations of the transverse size of the detonation cell in a suspension of aluminum particles in oxygen for particles of different fractions: the filled circles refer to uniform or close to uniform structures formed in wide channels (2.5 cells or more), the open circles show nonuniform structures, open diamonds refer to structures obtained in narrow channels (1–2 cells), and the curve shows dependence (9).

Examples of formation of uniform and close to uniform regular structures are shown in Fig. 6. For particles with $d = 3$ μm (Fig. 6a; $\Delta x = 0.001$ m), the structure is irregular only at the early stage of its formation; then it becomes regular and uniform and retains its character; the cell size is ≈4.3 cm. For particles with $d = 12$ μm, we have $\psi = 1.23$ for the channel width $Y = 1.4$ m (at the top of Fig. 6b) and $\psi = 1.1$ for $Y = 1.5$ m (at the bottom of Fig. 6b); the cell size lies in the interval of 35–37.5 cm ($\Delta x = 0.005$ m). The symmetry in terms of y in Fig. 6b for a monotonic initiating fluctuation (8) serves as additional evidence that the formation of cellular structures is an intrinsic property of the detonation process and is not determined by the initial fluctuation.

The calculations of the transverse size of the detonation cell λ are plotted in Fig. 7. The scatter of data decreases in passing from structures obtained in narrow channels (1–2 cells; open diamonds in Fig. 7) to nonuniform cellular structures (open circles) and then to uniform or close to uniform structures formed in rather wide channels (2.5 cells or more; filled circles), which again confirms reliability of results determined for uniform structures in rather wide channels.

The cell size of regular uniform structures (filled circles in Fig. 7) is approximately described by a power dependence on the particle diameter:

$$\lambda = \lambda_0 (d/d_0)^\theta. \qquad (9)$$

Here $\lambda_0 = 27$ cm for $d_0 = 10$ μm; the exponent is $\theta = 1.6$ (solid curve in Fig. 7).

The results obtained are in agreement with the experimental data of [14], where the formation of detonation cells 5–10 cm in size was observed in initiation of detonation in a mixture of spherical aluminum particles with $d = 3.5$ μm in oxygen. As is seen from Fig. 7, the transverse cell size for particles with $d = 3.5$ μm is 5 cm (correspondingly, the longitudinal size is about 10 cm). A comparison with the numerical data of [17] can be considered only as estimates because of the different initial content of particles and front velocity. The results for particles with $d = 2.5$ μm were obtained in [17] in a narrow channel (2 cells per channel width), and the change in the mode of cellular structures for particles with $d = 1$ μm in the process of front propagation shows that the chosen value of the width of the region corresponds to the bifurcation point. The structures formed thereby are characterized by nonuniformity and irregularity. In accordance with the data of [17], the cell size varies from 1.1 to 1.4 cm for particles with $d = 1$ μ and reaches ≈6 cm for particles with $d = 2.5$ μm.

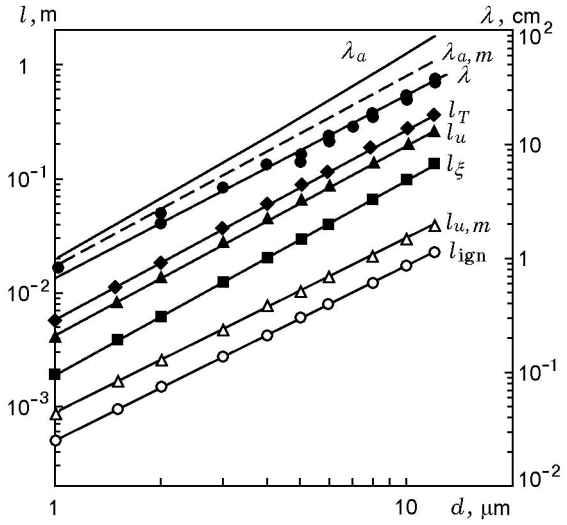

Fig. 8. Characteristic scales of the flow versus the particle size: λ is the calculated cells size, λ_a is the cell size estimates by an acoustic analysis of the self-sustained detonation wave, $\lambda_{a,m}$ is the minimum size of the detonation cell determined by an acoustic analysis of overdriven and decaying waves; l_T, l_u, $l_{u,m}$, l_ξ, and $l_{\rm ign}$ are the lengths of the thermal relaxation zone, significant and complete velocity relaxation zones, combustion zone, and ignition-delay zone, respectively.

RELATION BETWEEN THE CELL SIZE AND THE CHARACTERISTIC SCALES OF THE DETONATION STRUCTURE

It is difficult to determine the characteristic scales of relaxation and combustion zones in an unsteady flow with cellular detonation because of variability of the flow structure. The change in the maximum pressure at the front is 40 to 120 atm, which implies significant amplitudes of variation of temperature and, correspondingly, lengths of the ignition-delay zone, reaction zone, thermal relaxation zone, and velocity relaxation zone. Therefore, we used the approach accepted in gas detonation [9–11], where the characteristic size of the detonation cell is related to parameters and scales of the corresponding steady one-dimensional detonation wave. The solution of the problem of the structure of a steady detonation wave was obtained from a system of algebraic and ordinary differential equations, which follow from Eqs. (1)–(5) in a front-fixed coordinate system. The qualitative properties of steady solutions with allowance for velocity nonequilibrium were described in [24].

The characteristic spatial scales of the flow were found as follows. The length of the ignition-delay zone $l_{\rm ign}$ was determined as the distance from the front of the frozen SW to the point where $T = T_{\rm ign}$. The length of the combustion-reaction zone l_ξ was assumed to be the distance from the front to the point $|(\rho_2 - \rho_{2k})/\rho_{2k}| = \varepsilon$ (ρ_{2k} is the density of particles in the final equilibrium state and $\varepsilon = 5\%$). The process of velocity relaxation can be characterized by two scales: zone of significant velocity nonequilibrium $l_{u,m}$ and complete velocity relaxation l_u. This is related to the nonmonotonic behavior of the relative velocity $u_1 - u_2$, which is maximum at the front of the frozen SW, decreases to a certain negative minimum, increases again, and asymptotically approaches zero. (The velocity profiles in a steady detonation wave can be found, e.g., in [24].) Let us set the length $l_{u,m}$ as the distance from the front to the first point where $u_1 = u_2$. The lengths of the zones of complete velocity relaxation and thermal relaxation l_u and l_T are determined from the conventional criteria $|(u_1 - u_2)/u_0| \geqslant 3.3\%$ and $|(T_1 - T_2)/T_0| \geqslant 3.3\%$.

Figure 8 shows the calculated lengths of the zones of ignition delay and chemical, velocity, and thermal relaxation in a plane wave of steady detonation in a suspension of aluminum particles in oxygen. The calculated cell size of uniform (close to uniform) structures scaled accordingly are also plotted in this figure. All data can be approximated by straight lines, which indicates that these scales have power dependences on the particle size. The values of exponents for the scales are listed in Table 1.

As is seen from Fig. 8, the lengths of the ignition-delay zone $l_{\rm ign}$ and velocity-relaxation zone $l_{u,m}$ are close to each other, and the slopes of these curves coincide; it is seen from Table 1 that the values of $\theta_{\rm ign}$ and

TABLE 1

Exponents in the Dependences $l = Ad^{\theta}$ and $\lambda = Bd^{\theta}$

θ_{ign}	θ_{ξ}	$\theta_{u,m}$	θ_u	θ_T	θ_{λ}	θ_a	$\theta_{a,m}$
1.53	1.70	1.53	1.64	1.68	1.6	1.81	1.66

$\theta_{u,m}$ are close to 1.5. An analysis of formulas (4)–(6) shows that the intensity of thermal relaxation is proportional to $(2 + 0.6\text{Re}^{1/2}\text{Pr}^{1/3})/d^2$; therefore, in the region immediately behind the frozen SW, where the relative Reynolds number reaches the maximum value, the governing term is that containing $\text{Re}^{1/2}$, which finally defines the dependence of the length l_{ign} on the particle size as close to $d^2/\text{Re}^{1/2}$ or $d^{3/2}$.

The dependence of the combustion-zone length on the particle size has an exponent $\theta_{\xi} = 1.7$, which differs from 2, though we used the quadratic dependence on the particle diameter for τ_{ξ} in Eq. (3). This fact indicates that combustion of a suspension of particles in the detonation wave differs from combustion of a single particle under static conditions. By virtue of the Arrhenius law, the length of the combustion zone is affected by the thermal relaxation zone for which $\theta_T = 1.68$ (see Table 1) and, hence, $\theta_T < \theta_{\xi} < 2$. In turn, the process of thermal relaxation, in accordance with formulas (4)–(6), is related to the process of velocity relaxation, which is responsible for close values of θ_u and θ_T (see Table 1).

It is seen from the data in Fig. 8 and Table 1 that the exponent θ_{λ} in the dependence of the cell size on the particle diameter coincides with neither θ_{ign} nor θ_{ξ} but lies in the interval between them. This indicates that the cell size is not uniquely related to the length of any one of the two characteristic zones, namely, ignition-delay and combustion zones determining the gas-detonation cell, and both zones affect the size of the detonation cell formed. To obtain additional information, we performed computations with variation of ignition temperature and burning time of the particle. An increase in T_{ign} to 1200 K in a mixture of particles with $d = 3$ μm for a fixed value of τ_{ξ} leads approximately to a twofold increase in the length of the ignition-delay zone. In a channel 0.15 m wide, the structure formed contains 3.5 cells, as that in Fig. 6a, but this structure is nonuniform, i.e., with the cell size changed, this channel width approaches the bifurcation point. An increase in the ignition threshold leads to a decrease in the length of the ignition-delay zone, and the detonation-cell size decreases accordingly. Vice versa, an artificial increase in the value of τ_{ξ} increases the cell size of the structure being formed. Thus, as in gas detonation, the cell size here is affected by both the ignition-delay zone and the combustion zone, which, in turn, depend on the processes of particle heating and their deceleration in the gas flow, i.e., on the scales of thermal and velocity relaxation.

ESTIMATE OF THE CHARACTERISTIC CELL SIZE BY THE ACOUSTIC APPROACH

Barthel [9] proposed a method for estimating the characteristic transverse cell size as the distance between the neighboring transverse waves (or "hot spots" at the front). The method is based on the analysis of propagation of acoustic disturbances behind the detonation-wave front. Consideration of the transformation of the front of a diverging cylindrical wave in the field of a plane detonation flow $u(x)$ (in the front-fixed coordinate system) made it possible to construct a system of "frozen" rays, i.e., curves whose slope at each point corresponds to the direction of propagation of a segment of the front of a particular wave. Each ray is characterized by a constant σ, which is the apparent velocity of propagation of the wave front in the transverse direction. An analysis of the behavior of "frozen" rays shows that there are turning points in the field of the detonation flow, where the sign of propagation of the front segment in the x direction is changed; these points are determined by the condition $\sigma^2 = c^2 - u^2$, where c is the velocity of sound. Under the assumption that fluctuations from the combustion zone, which are the first ones to reach the front, are accumulated at hot spots, an expression for the transverse size of the detonation cell was derived:

$$\lambda_a = 4 \int_{x_1}^{x_2} \frac{c}{\sqrt{\sigma_*^2 - (c^2 - u^2)}}\, dx. \tag{10}$$

The limits of integration are determined as two points x_1 and x_2: the first point coincides with the front of the frozen SW and the second one corresponds to the ray turning point $\sigma_*^2 = c^2 - u^2$. The value of σ_* is chosen such that it ensures (for all σ) the minimum value of the time integral

$$t = 2 \int_{x_1}^{x_2} \frac{c\sigma}{(c^2 - u^2)\sqrt{\sigma^2 - (c^2 - u^2)}}\, dx. \tag{11}$$

The structure of the gas-detonation wave in the mixture considered in [9] (hydrogen–oxygen mixture diluted by argon) is characterized by a "plateau" in the distribution of the function $c^2 - u^2$ immediately behind the front (in the induction zone) and by a local maximum

in the combustion zone, followed by vanishing in the Chapman–Jouguet plane. For this reason, integral (11) diverges for $\sigma = \sigma_{\rm SW} = \sqrt{(c^2 - u^2)_{\rm SW}}$, where the subscript SW indicates the values immediately behind the front, and also diverges for $\sigma = \sigma_{\max} = \sqrt{(c^2 - u^2)_{\max}}$. Hence, in the interval $\sigma_{\rm SW} < \sigma < \sigma_{\max}$, there is a minimum of integral (11) reached for a certain value $\sigma = \sigma_*$, which was assumed to determine the cell size in the form (10). The results calculated in [9] for steady Chapman–Jouguet detonation are significantly higher than the experimentally observed values. It was possible to approach the experimental data by considering an overdriven detonation wave as the basic flow field; it turned out that the degree of overcompression has a nonmonotonic effect on the "acoustic" cell size. As the Mach number of the detonation wave increases, the cell size decreases, reaches a minimum, and then drastically increases and reaches a vertical asymptotic line. Good agreement between the characteristic transverse cell size calculated by the acoustic theory and experimental data in hydrogen–oxygen mixtures diluted by argon was obtained for moderately overdriven waves (the ratio of the Mach number to the Mach number at the Chapman–Jouguet point ranging from 1.05 to 1.2).

In the present work, the methodology of estimating the characteristic cell size [9] is applied to a detonation flow of a heterogeneous mixture of oxygen and aluminum particles. As the volume fraction of particles in a stoichiometric mixture is so small than allows us to neglect the influence of particles in the equation of state of the gas (2) and the terms depending on discrete-phase parameters are involved only into the right side of Eqs. (1), the characteristics of the system that describes the gas flow are determined by gas parameters only. The velocity of small fluctuations in the mixture equals the frozen velocity of sound in the gas $c_{\rm fr} = \gamma R T_1$, where $\gamma = 1 + R/c_{v,1}$. Hence, the influence of particles on propagation of acoustic fluctuations is manifested only in the change in the flow field of the gas and the distribution of $c_{\rm fr}$.

To apply the above-described methodology, we solved the problem of the structure of a steady detonation wave in a mixture of aluminum particles and oxygen. In this case, there are no Chapman–Jouguet regimes ($u_k = c_{\rm eq}$, where u_k is the velocity of the mixture in the final equilibrium state and $c_{\rm eq}$ is the equilibrium velocity of sound). Conventional self-sustained detonation corresponds to weak waves with an internal sonic point $u_1 = c_{\rm fr}$ [24] and a supersonic final equilibrium state. The Mach number of the velocity of self-sustained (weak) detonation with respect to the initial value of the velocity of sound in the gas is denoted here by $\mathrm{M}_w = D_w/c_{{\rm fr},0}$.

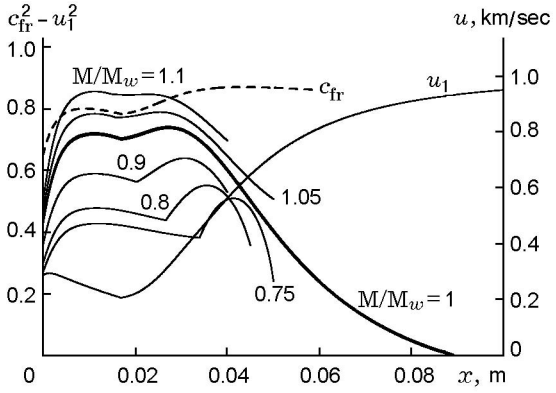

Fig. 9. Behavior of the characteristic functions in the structure of self-sustained, overdriven, and decaying detonation waves.

Let us note the following features of the flow field in the zone between the front of the frozen SW in the gas and the point $u_1 = c_{\rm fr}$, which distinguish this flow field from the gas-detonation flow [9]. The function $c_{\rm fr}^2 - u_1^2$ for the heterogeneous detonation wave has a more complicated character, which is associated with velocity and thermal relaxation of the phases. Figure 9 (bold curve) shows the distribution of $\psi(x) = c_{\rm fr}^2 - u_1^2$ for the self-sustained detonation wave in a mixture of 10-μm particles. In contrast to the "plateau" in the induction zone, which is typical of gas detonation [9], the function $\psi(x)$ first monotonically increases to a certain local maximum and then decreases to the ignition point. The behavior of the function $\psi(x)$ on this interval is determined by the character of the dependence $c_{\rm fr}(x)$ (dashed curve in Fig. 9). The initial growth of the velocity of sound behind the front of the frozen SW is caused by the growth of temperature due to heat release in the course of velocity relaxation. The subsequent small decrease occurs when the thermal relaxation of the phases starts to prevail and the gas temperature decreases owing to heat transfer to particles. After the beginning of the combustion reaction of particles behind the point of the local minimum, the behavior of $c_{\rm fr}^2 - u_1^2$ is similar to the function $c^2 - u^2$ described in detail in [9]. Here, $\psi(x)$ also increases (to the second point of the local maximum) and then decreases to zero, reached at $u_1 = c_{\rm fr}$. The only difference is that the transition through the point $u_1 = c_{\rm fr}$ in self-sustained detonation of suspended aluminum particles is observed before the chemical reaction is finished [24].

Thus, according to the results of [9], not all fluctuations from the combustion zone reach the leading front (and participate in formation of cells) but only those that propagate in a certain direction (determined by the

constant σ). Integral (11) here is defined on the segment including part of the combustion zone only if the value of σ is higher than the point of the first local maximum $\sigma_{\max,1} = \sqrt{(c_{\rm fr}^2 - u_1^2)_{\max,1}}$ but lower than the value of the second local maximum $\sigma_{\max,2} = \sqrt{(c_{\rm fr}^2 - u_1^2)_{\max,2}}$. Integral (2) diverges both for $\sigma = \sigma_{\max,1}$ and for $\sigma = \sigma_{\max,2}$. In the interval $\sigma_{\max,1} < \sigma < \sigma_{\max,2}$, the integral is finite; hence, it has a minimum reached at a certain value σ_*. Integral (10) for $\sigma = \sigma_*$ determines the characteristic transverse size of the detonation cell. The limits of integration for each value of σ within the indicated interval are determined in accordance with [9]: $x_1 = x_{\rm SW} = 0$ and $x_2 = x_{\sigma^2 = c_{\rm fr}^2 - u_1^2}$.

The calculated values of λ_a for the basic flow field corresponding to a self-sustained (weak) detonation wave are shown in Fig. 8. We can see that the value of λ_a is higher than λ; moreover, in the dependence $\lambda_a(d)$, the exponent $\theta_a = 1.81$ (see Table 1) differs from the exponent $\theta_\lambda = 1.6$ in Eq. (9), which is responsible for different slopes of the curves. Therefore, by analogy with [9], we considered overdriven detonation flows. It turned out that a change in the Mach number of the leading SW leads to a change in λ_a, but the qualitative dependence of λ_a on the degree of overcompression is different from that in gas detonation [9]. Figure 9 shows the distributions $\psi(x) = c_{\rm fr}^2 - u_1^2$ for the degree of overcompression $\mathrm{M}/\mathrm{M}_w = 1.05$ and 1.1. Here, as the SW Mach number increases, the first local maximum in the distribution $\psi(x)$ increases, and the value at the point of the first maximum becomes higher than that of the second maximum at $\mathrm{M}/\mathrm{M}_w > 1.04$. The value of λ_a monotonically increases and reaches a vertical asymptotic line. As in gas detonation, there exists a critical value of overcompression above which the acoustic theory is unable to predict the characteristic cell size. In a suspension of aluminum particles, the critical value M/M_w depends on the particle size and is close to unity. In the range of particle diameters considered (1–10 μm), the value of λ_a for overdriven regimes was found to be always higher than the value corresponding to the self-sustained (weak) mode.

Taking into account that the second phase of propagation of the cellular detonation front is a decaying wave, we also considered propagation of fluctuations in the flow field of decaying detonation. The flow parameters were determined within the quasi-steady approximation, which yields a system of ordinary differential equations whose solution exists on a limited interval from the front of the frozen SW to the flow choking line $u_1 = c_{\rm fr}$. The corresponding distributions $\psi(x)$ for $\mathrm{M}/\mathrm{M}_w = 0.9$, 0.8, and 0.75 are also plotted in Fig. 9. As the Mach number decreases, the induction zone increases, and the maximum values decrease; the value of the first local maximum decreases faster than the value of the second local maximum. As a result, with decreasing M/M_w, the value of λ_a decreases, reaches a certain minimum value in the interval $0.78 < \mathrm{M}/\mathrm{M}_w < 0.8$, and then increases again. (The values of M/M_w below 0.75 were not considered.) The minimum values $\lambda_{a,m} = \min\limits_{\mathrm{M}}(\lambda_a)$ for different fractions of particles are shown in Fig. 8 (dashed curve). They lie closer to the values of numerical experiments; moreover, the exponent in the dependence $\lambda_{a,m}(d)$ is $\theta_{a,m} = 1.66$, which is close to the corresponding exponent $\theta_\lambda = 1.6$ (see Table 1). Thus, the estimates of the characteristic cell size obtained in the acoustic approximation agree with the results of numerical experiments on formation of cellular detonation in channels both quantitatively and qualitatively.

The analysis performed confirms the influence of the characteristic scales of all processes proceeding in the mixture on the characteristic cell size. Simultaneous proceeding of velocity and thermal relaxation determines the magnitude and position of the point of the first local maximum in the dependence $c_{\rm fr}^2 - u_1^2$; the position of the point of the local minimum is determined by ignition conditions; simultaneous proceeding of thermal relaxation and combustion determines the positions of the turning points of the "frozen" rays and the magnitude of the second local maximum.

Thus, an analytical approach based on an analysis of propagation of acoustic fluctuations also confirms that the cell size in heterogeneous detonation is related to the characteristic scales of all relaxation processes in the mixture, including not only ignition and combustion of particles but also thermal and velocity relaxation of the phases.

CONCLUSIONS

Formation of cellular structures in channels with shock-wave initiation is numerically simulated within the framework of the physicomathematical model of heterogeneous detonation of a suspension of aluminum particles in oxygen, which was verified by available experimental data.

By varying the width of the computational domain and comparing the character of the structures, the numerical values of the characteristic transverse cell size are determined. By comparing the results computed on two different grids by two different methods, it is established that reliable values of the cell size are determined in channels of sufficiently large width (several cells) on the basis of regular uniform structures.

The dependences of the calculated cell size and characteristic scales of a steady one-dimensional wave of self-sustained detonation are determined to be power functions of the particle size. A comparative analysis of the exponents in these dependences allows us to conclude that the basic scales in formation of cells are zones characterizing chemical processes: ignition delay and combustion. In turn, these scales in heterogeneous detonation are related to velocity and thermal relaxation processes.

The characteristic size of the detonation cell is estimated by an acoustic analysis. These estimates are in good agreement with the data of numerical experiments in terms of both the magnitude and the exponent in the dependence on the particle size. Typical features of the structure of the heterogeneous detonation wave are indicated, which confirm that the cell size is affected by the characteristic scales of velocity and thermal relaxation of the phases.

This work was supported by the Russian Foundation for Basic Research (Grant No. 03-01-00453).

REFERENCES

1. R. A. Strechlov, "Gas phase detonations: Recent developments," *Combust. Flame*, **12**, No. 2, 81–101 (1968).
2. A. A. Vasil'ev, V. V. Mitrofanov, and M. E. Topchiyan, "Detonation waves in gases," *Combust., Expl., Shock Waves*, **23**, No. 5, 605–623 (1987).
3. E. Oran, "The structure of propagating detonation," in: G. Roy et al. (eds.), *Gaseous and Heterogeneous Detonations*, ENAS, Moscow (1999), pp. 97–120.
4. M. A. Nettleton, "Recent work on gaseous detonations," *Shock Waves*, **12**, No. 1, 3–12 (2002).
5. K. I. Shchelkin and Ya. K. Troshin, *Gas-Dynamics of Combustion* [in Russian], Izd. Akad. Nauk SSSR, Moscow (1963).
6. V. V. Mitrofanov, *Theory of Detonation* [in Russian], Novosibirsk Univ., Novosibirsk (1982).
7. A. A. Vasil'ev and Yu. A. Nikolaev, "Model of the nucleus of a multifront gas detonation," *Combust., Expl., Shock Waves*, **12**, No. 5, 667–674 (1976).
8. D. Desbordes, "Transmission of overdriven plane detonations: Critical diameter as a function of cell regularity and size," in: *Progress in Astronautic and Aeronautic*, Vol. 114: *Dynamics of Explosions*, AIAA Inc., New York (1988), pp. 170–185.
9. H. O. Barthel, "Predicted spacings in hydrogen-oxygen-argon detonations," *Phys. Fluids*, **17**, No. 8, 1547–1553 (1974).
10. J. E. Shepherd, "Chemical kinetics of hydrogen-air-diluent detonations," in: *Progress in Astronautic and Aeronautic*, Vol. 106: *Dynamics of Explosions*, AIAA Inc., New York (1985), pp. 263–293.
11. A. I. Gavrikov, A. A. Efimenko, and S. B. Dorofeev, "A model for detonation cell size prediction from chemical kinetics," *Combust. Flame*, **120**, 19–33 (2000).
12. B. A. Khasainov and B. Veyssiere, "Initiation of detonation regimes in hybrid two-phase mixtures," *Shock Waves*, **6**, 9–15 (1996).
13. B. Veyssiere and W. Ingignoli, "Existence of the detonation cellular structure in two-phase hybrid mixtures," *Shock Waves*, **12**, 291–299 (2003).
14. W. Ingignoli, B. Veyssiere, and B. A. Khasainov, "Study of detonation initiation in unconfined aluminum dust clouds," in: G. Roy et al. (eds.), *Gaseous and Heterogeneous Detonations*, ENAS, Moscow (1999), pp. 337–350.
15. F. Zhang and H. Grönig, "Transition and structure of dust detonations," in: A. A. Borisov (ed.), *Dynamic Structure of Detonation in Gaseous and Dispersed Media*, Kluwer Academic Publ. (1991), pp. 157–213.
16. B. A. Khasainov, B. Veyssiere, and W. Ingignoli, "Numerical simulation of detonation cell structure in hydrogen–air mixture loaded by aluminum particles," in: G. Roy et al. (eds.), *High-Speed Deflagration and Detonation, Fundamental and Control*, ELEX-KM, Moscow (2001), pp. 163–174.
17. K. Benkiewicz and A. K. Hayashi, "Two-dimensional numerical simulations of multi-headed detonations in oxygen-aluminum mixtures using an adaptive mesh refinement," *Shock Waves*, **13**, 385–402 (2003).
18. A. A. Borisov, B. A. Khasainov, B. Veyssiere, et al., "Detonation of aluminum suspensions in air and oxygen," *Khim. Fiz.*, **10**, No. 2, 250–272 (1991).
19. M. Nikolis, D. N. Williams, and L. Bauwens, "Simulation of detonation cells in wide channel," in: G. Roy et al. (eds.), *Gaseous and Heterogeneous Detonations*, ENAS, Moscow (1999), pp. 153–162.
20. L. Hemeryck, M. N. Lefebre, and P. J. Van Tiggelen, "Numerical investigation of transient detonation waves," in: G. Roy et al. (eds.), *High-Speed Deflagration and Detonation. Fundamental and Control*, ELEX-KM, Moscow (2001), pp. 81–96.
21. W. A. Strauss, "Investigation of the detonation of aluminum powder–oxygen mixtures," *AIAA J.*, **6**, No. 12, 1753–1761 (1968).
22. A. E. Eremeeva, A. V. Medvedev, A. V. Fedorov, and V. M. Fomin, "On the theory of ideal and nonideal detonation of aerosuspensions," Preprint No. 37–86, Inst. Theor. Appl. Mech., Sib. Div., Acad. of Sci. of the USSR, Novosibirsk (1986).
23. A. V. Fedorov, "Structure of heterogeneous detonation of aluminum particles dispersed in oxygen," *Combust., Expl., Shock Waves*, **28**, No. 3, 277–286 (1992).

24. A. V. Fedorov, V. M. Fomin, and T. A. Khmel', "Non-equilibrium model of steady detonations in aluminum particle-oxygen suspensions," *Shock Waves*, **9**, No. 5, 313–318 (1999).
25. A. V. Fedorov and T. A. Khmel', "Numerical simulation of shock-wave initiation of heterogeneous detonation in aerosuspensions of aluminum particles," *Combust., Expl., Shock Waves*, **35**, No. 3, 288–295 (1999).
26. T. A. Khmel' and A. V. Fedorov, "Numerical simulation of detonation initiation with a shock wave entering a cloud of aluminum particles," *Combust., Expl., Shock Waves*, **38**, No. 1, 101–108 (2002).
27. T. A. Khmel' and A. V. Fedorov, "Interaction of a shock wave with a cloud of aluminum particles in a channel," *Combust., Expl., Shock Waves*, **38**, No. 2, 206–214 (2002).
28. E. L. Dreizin, "On the mechanism of asymmetric aluminum particle combustion," *Combust. Flame*, **117**, 841–850 (1999).
29. V. M. Boiko, V. P. Kiselev, S. P. Kiselev, et al., "Interaction of a shock wave with a cloud of particles," *Combust., Expl., Shock Waves*, **32**, No. 2, 191–203 (1996).
30. A. Harten, "High resolution schemes for hyperbolic conservation laws," *J. Comp. Phys.*, **49**, No. 3, 357–393 (1983).
31. P. J. Roache, *Computational Fluid Mechanics*, Hermosa, Albuquerque (1976).
32. T. A. Khmel', "Numerical simulation of two-dimensional detonation flows in a gas suspension of reacting solid particles," *Mat. Model.*, **16**, No. 6, 73–77 (2004).